Taylor & Francis
Taylor & Francis Group

Check for updates

Design and *in silico* study of the novel coumarin derivatives against SARS-CoV-2 main enzymes

Mücahit Özdemir[a] (iD), Baybars Köksoy[b] (iD), Deniz Ceyhan[c] (iD), Koray Sayın[d,e] (iD), Erol Erçağ[c] (iD), Mustafa Bulut[a] (iD) and Bahattin Yalçın[a] (iD)

[a]Department of Chemistry, Marmara University, Istanbul, Turkey; [b]Department of Chemistry, Bursa Technical University, Bursa, Turkey; [c]Department of Chemistry, Tekirdağ Namık Kemal University, Tekirdağ, Turkey; [d]Department of Chemistry, Sivas Cumhuriyet University, Sivas, Turkey; [e]Advanced Technology Research and Application Center, Sivas Cumhuriyet University, Sivas, Turkey

Communicated by Ramaswamy H. Sarma

ABSTRACT

The novel coronavirus (SARS-CoV-2) causes severe acute respiratory syndrome and can be fatal. In particular, antiviral drugs that are currently available to treat infection in the respiratory tract have been experienced, but there is a need for new antiviral drugs that are targeted and inhibit coronavirus. The antiviral properties of organic compounds found in nature, especially coumarins, are known and widely studied. Coumarins, which are also metabolites in many medicinal drugs, should be investigated as inhibitors against coronavirus due to their pharmacophore properties (low toxicity and high pharmacokinetic properties). The easy addition of substituents to the chemical structures of coumarins makes these structures unique for the drug design. This study focuses on factors that increase the molecular binding and antiviral properties of coumarins. Molecular docking studies have been carried out to five different proteins (Spike S1-subunit, NSP5, NSP12, NSP15, and NSP16) of the SARS-CoV-2 and two proteins (ACE2 and VKORC1) of human. The best binding scores for 17 coumarins were determined for NSP12 (NonStructural Protein-12). The highest score (–10.01 kcal/mol) in the coumarin group is 2-morpholinoethan-1-amine substituted coumarin. Molecular mechanics Poisson-Boltzmann surface area (MM-PBSA) analyses of selected ligand-protein complexes were performed. The binding energies in each 5 ns were calculated and it was found that the interaction between ligand and target protein were stable.

Abbreviations: ACE2: Angiotensin-Converting Enzyme 2; B3LYP: Becke's three-parameter nonlocal exchange functional Lee-Yang-Parr's correlation function; COVID-19: Coronavirus Disease 20,192,019; ESP: Electrostatic Potential; HOMO: Highest Occupied Molecular Orbital; LUMO: Lowest Unoccupied Molecular Orbital; MM-PBSA: Molecular Mechanics-Poisson Boltzman Surface Area; MOE: Molecular Operating Environment; MPro: Main Protease; nCoV: 2019 novel Coronavirus; NSP: Nonstructural Protein; PDB: Protein Data Bank; RdRp: RNA-dependent RNA polymerase; RMS: Root Mean Deviation; RNA: Ribonucleic Acid; SARS-CoV-2: Severe Acute Respiratory Syndrome Coronavirus 2; SCF: Self-Consistent Field; VKORC1: Vitamin K epOxide Reductase Complex subunit 1; WHO: World Health Organization

1. Introduction

When the coronavirus first appeared in Wuhan, Hubei province, China in December 2019, its source was unknown and traces of pneumonia were visible in patients carrying the virus (Huang et al., 2020; Lu et al., 2020; Zu et al., 2020). This virus, which was found to belong to the coronavirus family, was first named 2019-nCoV (2019-novel CoronaVirus), and then the World Health Organization changed this name to SARS-CoV-2 (Severe Acute Respiratory Syndrome-Corona Virus-2) due to its close similarity to SARS-CoV (Gorbalenya et al., 2020; Guo et al., 2020). The disease caused by the coronavirus (COVID-19) is highly contagious and spreads rapidly from person to person. Since the virus spread rapidly all over

the world, it has been declared a global pandemic by the WHO (Ghebreyesus, 2020).

COVID-19 affects people in various ways and no generalization can be made. Many people infected with the virus have mild to moderate symptoms and recover without hospitalization (Al-Tawfiq, 2020). In severe cases, common symptoms include respiratory distress, fever, weakness, dry cough, shortness of breath, headache, and pain of the bones (Singhal, 2020). The group in which the symptoms of the disease are most effective are those with diabetes, heart, cancer, hypertension, and chronic respiratory diseases (Casey et al., 2020; Fang et al., 2020; Ganatra et al., 2020; Kreutz et al., 2020; Zheng et al., 2020). For patients included in the risk group, coronavirus is very dangerous and in advanced

cases, the infection can cause pneumonia, acute respiratory failure, kidney failure, pulmonary embolism, and even death (Jordan et al., 2020; X. Wang et al., 2020). Coronavirus effects can be prevented by inhibiting the binding of the virus to human cell receptors, the spread of their genetic material, and the replication. Several antiviral drug combinations have been tried for the treatment of COVID-19, but it has been reported that these drugs are not excellent effective. Many scientists around the world are researching to discover new drugs for inhibition of coronavirus. Phytochemicals, as well as normal chemical drugs against SARS-CoV-2, are tested and satisfactory results are obtained (Chikhale et al., 2020; da Silva Antonio et al., 2020; Kumar et al., 2020; Pandey et al., 2020; Ul Qamar et al., 2020).

Coumarins are natural organic phytochemicals found in some plants as well as easily synthesized (Murray et al., 1982). As a result of extensive research, antiviral, anticoagulant, antibacterial, and anticancer properties have been proven (de Souza et al., 2005; Hassan et al., 2016; Koch-Weser & Sellers, 1971; Sashidhara et al., 2010; Thakur et al., 2015). For example, warfarin (coumadin) is used as a vitamin K-antagonist for cardiac patients (warfarin achieves its anticoagulant effect by competitive inhibition with vitamin K epoxide reductase) and it has been proven by experiments that it does not have a high toxic effect in clinical studies. The excellent pharmacophore properties of coumarins make this group prominent in drug design.

Coronaviruses are enveloped, single-stranded, positive RNA viruses that have been almost completely analyzed, all their receptors published in the protein data bank (PDB). SARS-CoV-2 contains two characteristic protein groups and accessory factors. The first is structural proteins and consist of the Spike (S), Membrane (M), Nucleocapsid (N), and Envelope (E) protein group. The second is non-structural proteins, and consist of the NSP1, NSP2, NSP3 (Papain-like), NSP4, NSP5 (Main protease, 3CLpro), NSP6, NSP7, NSP8, NSP9 (RNA replicase), NSP10, NSP11, NSP12 (RNA-dependent RNA polymerase-RdRp), NSP13 (Helicase), NSP14 (Exonuclease), NSP15 (NendoU), NSP16 (2'O-Methyltransferase). The main protease cleaves at 11 sites within the polyprotein to release NSP4-NSP16. It is also responsible for NSP maturation (Wu et al., 2020). The spike protein is split into glycosylated subunits (S1 and S2). S1 binds to host receptor ACE2 while S2 mediates viral and host membrane fusion (Hoffmann et al., 2020). NSP12 is an RNA-dependent RNA polymerase (RdRp) that performs both replication and transcription of the viral genome (Q. Wang et al., 2020). NSP15 is an endoribonuclease that promotes cleavage of RNA at the 3'-ends of uridylates. Loss of NSP15 affects both viral replication and pathogenesis. It is also necessary to avoid host cell dsRNA sensors (Kim et al., 2020). NSP16 interacts with the NSP10 and is activated. 2'-O-methyltransferase activity is required for viral mRNA capping. It can also work against host cell antiviral sensors (Viswanathan et al., 2020). Human Angiotensin converting enzyme 2 (hACE2) is an enzyme bound to the cell membranes of cells in the lungs, arteries, heart, kidney and intestines (Donoghue et al., 2000; Hamming et al., 2004). ACE2 catalyzes the conversion of angiotensin II to angiotensin by hydrolysis and lowers blood pressure (Keidar et al., 2007). ACE2 interacts with spike proteins around the coronavirus, is entry point and allows the virus to enter the cell (Cao et al., 2020). Vitamin K epOxide Reductase protein complex is responsible for its reduction to the active form of vitamin K 2,3-epoxide, which is important for coagulation. As a result of the inhibition of VKORC1, vitamin K-hydroxylation cannot become active and coagulation does not occur (Czogalla et al., 2015; Oldenburg et al., 2006).

The reason for the selection of secondary amine-containing coumarins in this study is that coumarins are natural, easy to synthesize and derivatize, have high biological activity and low toxicity, and such an important group has been scarcely investigated for SARS-CoV-2. Molecular docking studies, which are the first step of drug design, have been carried out on target coumarins, and the high score results we have obtained will be a stepping stone for scientists who will conduct *in vitro* and *in vivo* studies.

MM-PBSA analysis is significant to determine the relationship between drug candidate and target protein. In this analysis, the interaction energy can be calculated in picosecond level to evaluate the stability of drug – protein complex (Aktaş et al., 2020). MM-PBSA analyses between coumarins **3**, **5**, **16** and remdesivir are performed by using nanoscale molecular dynamics (NAMD) and visual molecular dynamics (VMD) software.

2. Experimental section

2.1. Materials and equipment

2.1.1. Coumarins
Ethyl 7-Hydroxy-4,8-dimethylcoumarin-3-propanoate (**1**) can be synthesized according to the synthesis method in the literature (Abuknesha & Darwish, 2005). Amide structure is obtained by nucleophilic reaction of ethyl carboxylate moiety of 7-hydroxy-4,8-dimethylcoumarin-3-propanoate (**1**) compound with free amines. *N*,*N*-dimethylethylenediamine (for **2**), 4-(2-aminoethyl)morpholine (for **3**), 1-(2-aminoethyl)piperidine (for **4**), 1-(2-aminoethyl)piperazine (for **5**), propan-1-amine (for **6**), aniline (for **7**), pyridin-4-amine (for **8**), 1*H*-imidazol-2-amine (for **9**), 2-aminobenzimidazole (for **10**), 2-aminooxazole (for **11**), 2-aminobenzoxazole (for **12**), 5-aminoindole (for **13**), 2-amino-1,9-dimethyl-1,9-dihydro-6*H*-purin-6-one (for **14**), cytosine (for **15**), 5,6-dihydro-3*H*-purin-6-amine (for **16**) and 2-aminobenzothiazole (for **17**) were used for amidation reaction of 7-hydroxy-4,8-dimethylcoumarin-3-propanoate (Scheme 1).

2.1.2. Molecular docking studies
Molecular docking studies were conducted to provide a theoretical perspective for possible molecular interactions of compounds with the target proteins. The theoretical binding affinities of these compounds for targeted proteins were also determined by docking calculations. Molecular docking calculations, energy minimization, and molecular visualization of docking results were carried out by using the Molecular Operating Environment software package (MOE, v2019.0102,
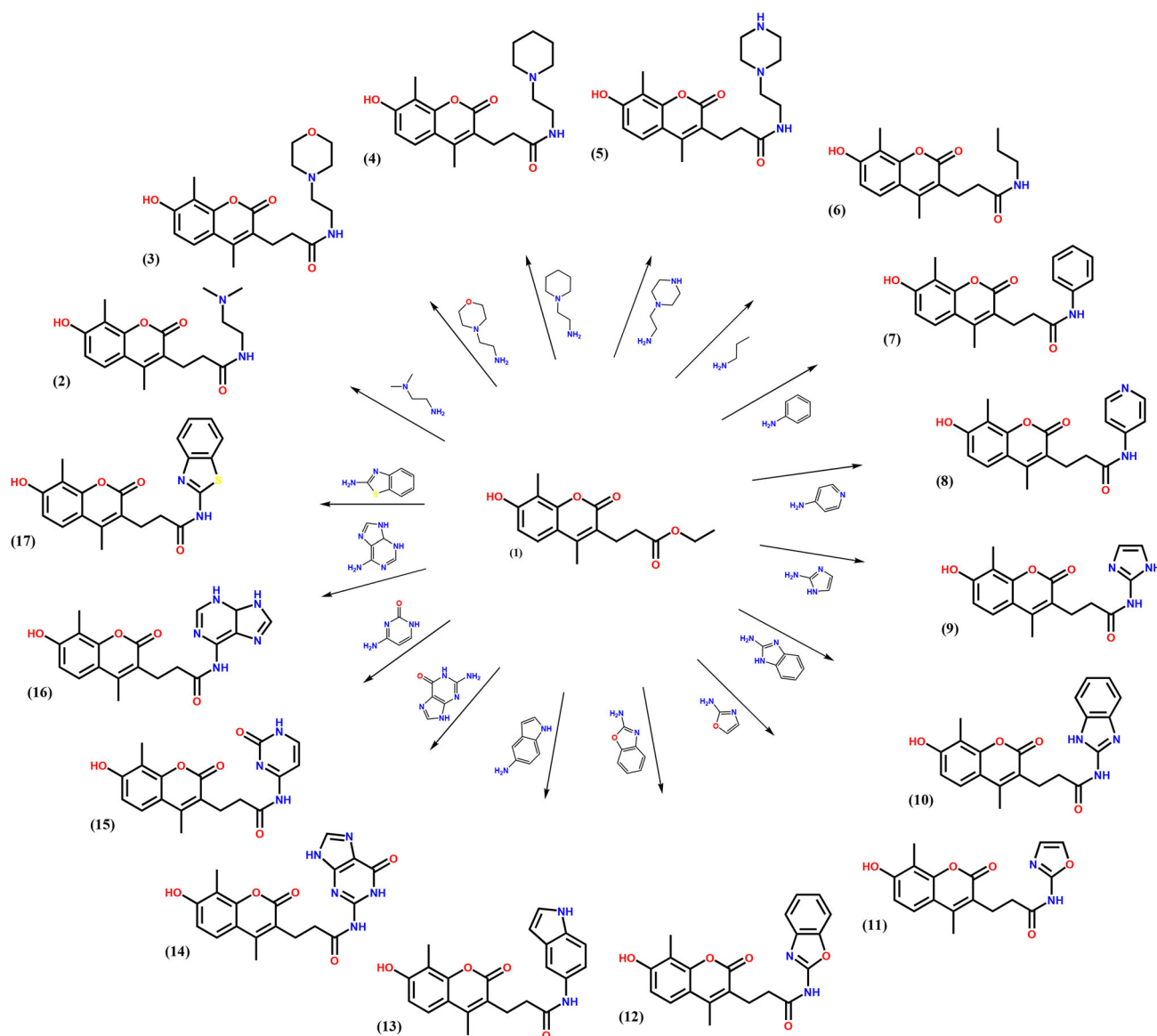
Scheme 1. Representation of ethyl 7-hydroxy-4,8-dimethylcoumarin-3-propanoate (**1**) and its amido derivatives (**2-17**).

Chemical Computing Group ULC) (ULC, 2019). Preparation of coumarin derivatives (**1-17**) compounds and model inhibitor molecules for molecular docking was performed with MarvinSketch software (ChemAxon, 2016). Before the docking process, the drawing and editing of the newly designed coumarin compounds in the SD File format were done with the MarvinSketch suit program (ChemAxon, 2016). These molecular structures have been protonated, were charges added, and conformation minimization was performed with the root mean square gradient (RMS 0.001 kcal/mol/A2) by using the MMFF94 Forcefield parameters, which can be accessed in Energy Minimization protocols of this software (Halgren, 1996). In this study, docking analyzes of coumarin derivatives (**1-17**) for 7 target proteins were performed. Of these target proteins Spike S1 subunit, NSP5, NSP12, NSP15, and NSP16 are COVID-19 proteins, ACE2 and VKORC1 are human proteins. The VKORC1 target protein is not directly related to COVID-19, but is involved in vitamin K-metabolism. Since it is the natural potential target protein for the coumarin

derivatives we have developed, it has been subject to study. In docking calculations, the homology model with UniProtKB-code-Q9BQB6-in SWISS-MODEL-repository was used for the VKORC1 3 D protein structure (Bienert et al., 2017; Consortium, 2019). Favipiravir is effective against coronavirus proteins due to its covalent interaction, coumarins containing morpholine, piperidine and piperazine exhibit NH^+ or NH_2^+ ionic interaction, (Since HOMO orbitals are on amide derivatives and LUMO orbitals are on the coumarin structure, electrons migrate from the substituent to the main skeleton). As shown in their calculations, it is important that NSP12 has the potential to covalently bond with RNA components, similar to favipiravir. This indicates that compounds with NH^+ properties may have an irreversibly strong inhibitory effect on NSP12-RNA. It will be important to demonstrate experimentally at the next stage (for HOMO-LUMO, Figure 3 and for NH^+ ionic interaction of compound **3**, Figure 4). The X-ray crystal structures as three-dimensional coordinates of these target proteins were obtained from the
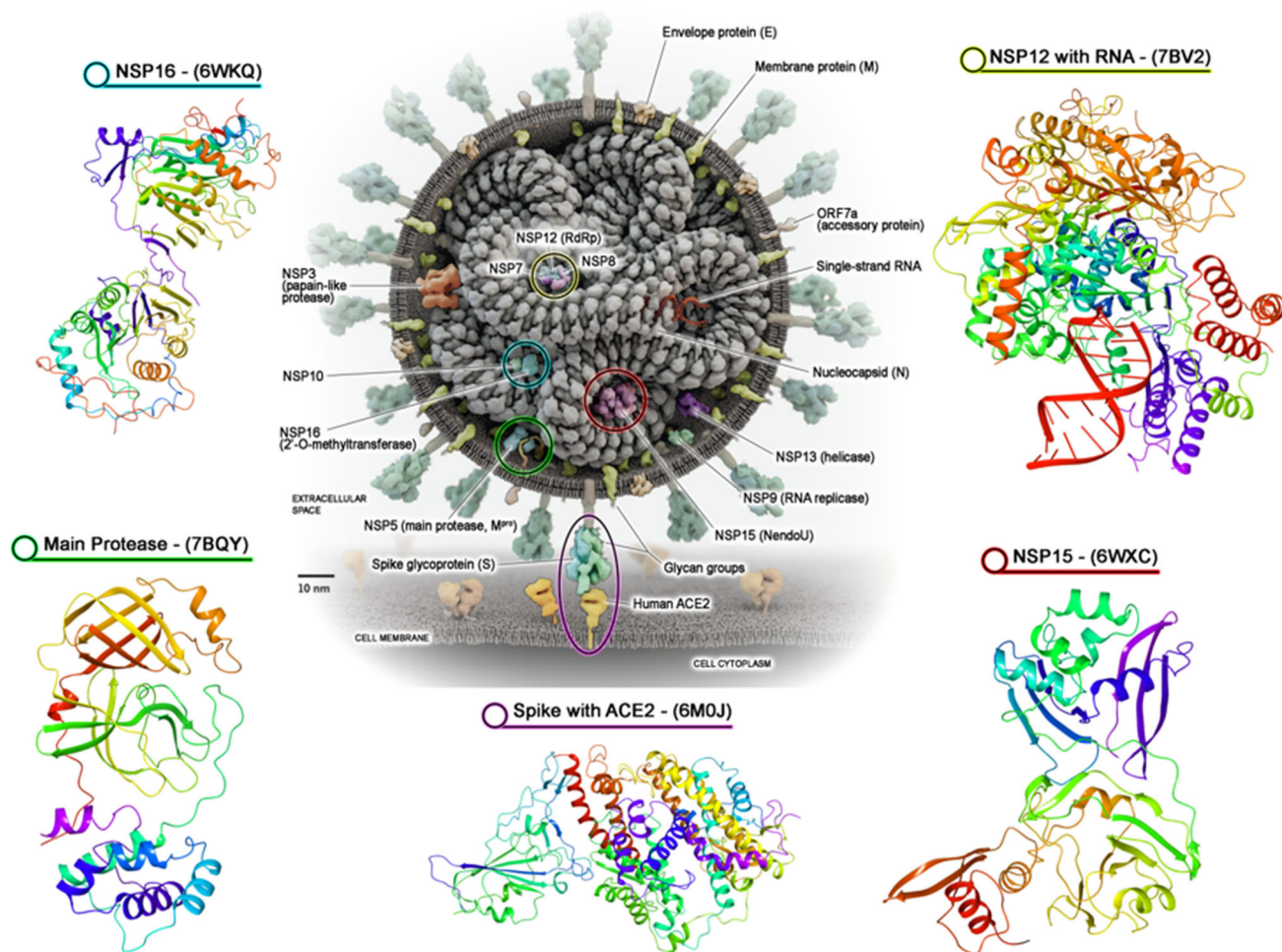
Figure 1. SARS-CoV-2 structure and related proteins in this study. Corona virus 3D image from (Parks & Smith, 2020).

Research Collaboratory for Structural Bioinformatics (RCSB) Protein Data Bank (http://www.rcsb.org/) (Berman et al., 2000). For use in docking calculations, structures with PDB IDs of 7BQY (Jin et al., 2020) for 3CLpro, 7BV2 (Yin et al., 2020) for NSP12, 6WXC (Kim et al., 2020) for NSP15, 6WKQ (Minasov et al., 2020) for NSP16, and 6M0J (Lan et al., 2020) for Spike S1 subunit and ACE2 protein were chosen as crystal structure models corresponding to these target proteins (Figure 1).

Structural defects in these target proteins were eliminated automatically with the "Structure Preparation" module of MOE suit software. Default parameters of MOE Protonate 3D Module were used to determine and optimize the overall low potential energy configuration of the terminal amides, hydroxyls, thiols, histidines, and hydrogenation positions of the titratable groups in a certain pH throughout the system (Temperature 300 K, pH 7, solvent 0.1 M, electrostatic energy cutoff 15 A with Generalized Born Model_GB/VI; van der Waals 800R3 cutoff 10 A, MOE Protonate 3D) (Lan et al., 2020). The energy minimization of the system was performed with the Amber12: EHT Forcefield parameters, RMS with the gradient of 0.001 kcal/mol/A2, which can be reached in MOE Energy Minimization protocols (Case et al., 2012; Labute, 2007). Possible ligand binding sites in the minimized protein were determined by MOE' SiteFinder module. The Site Finder

methodology is a geometric method based on Alpha Shapes, a generalization of convex surfaces developed by Edelsbrunner (Gerber & Müller, 1995).

Local docking of coumarin compounds (**1-17**) and model inhibitors to the active site of these targets proteins was performed via MOE using the default docking calculation parameters. The top-ranked pose defined by minimum energy (kcal/mol) for every compound, was used as the final molecular docking results. London ΔG scoring function was used for docking calculations. The London ΔG scoring function estimates the free energy of binding the ligand at a particular pose in a target structure. This scoring function is explained in detail in the user manual of the MOE software. After the initial scoring function for the obtained docking poses, the GBVI/WSA ΔG scoring function was used as the final docking scoring methodology. The GBVI/WSA ΔG is a forcefield-based scoring function that estimates the free energy of binding of the ligand from a given pose (Edelsbrunner & Mücke, 1994). This scoring function is explained in detail in the user manual of the MOE software.

2.1.3. DFT calculations

The Gaussian 09 (Frisch et al., 2009) program was used to perform theoretical calculations, and the computational

results were visualized through GaussView 5.0 (Dennington et al., 2009). The B3LYP functional [B3: Becke's three-parameter nonlocal exchange functional, (Becke, 1988, 1993) LYP: Lee-Yang-Parr's correlation function (Lee et al., 1988)] was used for density functional theory (Kohn & Sham, 1965) with the 6-311 G(d,p) basis set. Geometry optimization was carried out in the gas phase. For geometry optimization of the compounds was chosen as a stable form with C1 symmetry. Also, frequency analysis of coumarins was performed. Total SCF Density (isoval = 0.0004 e/au^3) mapped with electrostatic potential (ESP) was utilized to visualize the total electron density.

2.1.4. Admet predictions

In drug design, the estimation of the pharmacophore properties of the target molecules saves time. ADMET is an acronym for absorption, distribution, metabolism, excretion, and toxicity, and a pharmacophore is an approach that offers parameters about the placement of a compound into a living organism. All of these five criteria determine the pharmacological activity of the compounds. pkCSM, a free online web server (http://structure.bioc.cam.ac.uk/pkcsm) (Pires et al., 2015) was used to predict the ADMET properties of the designed coumarin derivatives (1–17).

2.1.5. MM-PBSA calculations

Molecular mechanics Poisson-Boltzmann surface area (MM-PBSA) calculations were performed for coumarins 3, 5, 16 and Remdesivir. Binding free energies were determined for these ligand–protein structures in 7BV2 from 0 to 100 ns (Kollman et al., 2000). For these calculations, Nanoscale Molecular Dynamics (NAMD) (Nelson et al., 1996) and Visual Molecular Dynamics (VMD) (Humphrey et al., 1996) software were used. Binding energy was calculated by using Equation (1).

$$\Delta G_{Binding} = G_{Complex} - G_{Protein} - G_{Ligand} \qquad (1)$$

where $\Delta G_{Binding}$ is the binding free energy, $G_{Complex}$, $G_{Protein}$, and G_{Ligand} demonstrates the total free energy of the protein-ligand complex and total free energies of the isolated protein and ligand, respectively.

3. Results and discussion

3.1. DFT studies

Ethyl 7-hydroxy-4,8-dimethylcoumarincoumarin-3-propanamido coumarin derivatives designed for the inhibition of SARS-CoV-2 proteins have been optimized by B3LYP/6-311G (d,p) level of theory. Possible molecular geometries of coumarins are shown in Figure 2.

Electronic energy values for all designed coumarin compounds increased negatively as secondary amines were added to the structure compared to the main coumarin structure 1 (Figure 3). This indicates that the secondary amine addition to the coumarin structure makes the structure more active. The largest electronic energy value −27128.87 kcal/mol for ethyl 7-hydroxy-4,8-

dimethycoumarinl-3-propanoate (1). The lowest electronic energy value is −44083.76 kcal/mol for 7-hydroxy-4,8-dimethyl-3-N-(benzo[d]thiazol-2-yl)-propanamido-coumarin (17).

HOMO (Highest Occupied Molecular Orbital) and LUMO (Lowest Unoccupied Molecular Orbital) energy levels, and the gap value between these two orbitals provide information about electronic transitions for the target molecules and are very important parameters. Also, the HOMO and LUMO values show nucleophilic and electrophilic attraction in the molecule as well as electronic transitions. The band gap (HOMO-LUMO gap) is a parameter that gives information about chemical reactivity and a narrow band gap means high reactivity and a wide band gap means lower reactivity according to the relevant molecule groups. Very useful for comparing chemical reactivity of compounds in a series. Band gaps were lowered by substituting secondary amines into ethyl 7-hydroxy-4,8-dimethylcoumarin-3-propanoate coumarin (1).

3.2. Molecular docking studies

Docking analyzes were performed to understand the molecular interaction mechanisms between coumarin derivatives (1-17) and the target proteins. Also of these, docking analyzes of model inhibitor warfarin and some drugs (favipiravir, hydroxychloroquine, and remdesivir) reported to be effective against COVID-19 were also performed (Barnes et al., 2020; Beigel et al., 2020; Cai et al., 2020; Gautret et al., 2020; Geleris et al., 2020; Grein et al., 2020; Y. Wang et al., 2020). Docking results of all compounds are given in Tables 1, 2, and Figures 4, 5, S1–S4 (Supporting material). According to docking calculations between the coumarin compound series (1-17) and NSP12, the compounds presenting the highest docking scores are 3, 5, and 16 with average binding affinities of −10.01, −9.36, and −9.09 kcal mol^{-1}, respectively. The binding affinities of these compounds to NSP12-RNA complex are −8.30, −9.10, and −8.39 kcal/mol, respectively.

The catalytic site major residues of NSP12 that interact with coumarin compounds (1-17) are Asp452, Tyr455, Met542, Arg553, Arg555, Thr556, Asp618, Tyr619, Pro620, Lys621, Cys622, Asp623, Arg624, Thr680, Ser 681, Ser682, Asn691, Phe694, Ser759, Asp760, Ser795. NSP12 (PDB ID: 7BV2) has magnesium ions in its catalytic domain. Since magnesium ions take part in natural catalytic processes, they are preserved in docking calculation and considered as a catalytic site component (as residues MG1004 and MG1005). It was seen in docking calculation that these magnesium ions, especially MG1004, form metal ligation with all coumarin compounds (1-17).

The residues of the NSP12 protein that show the highest interaction with coumarins (1-17) are Asp623, Thr556, Ly621, and Pro620, respectively. Asp623 and Thr556 residues usually show strong sidechain hydrogen bond (donor) interaction in different docking poses of coumarin compounds (1-17). When the different docking poses of coumarin derivatives with NSP12 were examined together, it was observed that the Lys621 residue had strong sidechain hydrogen bond
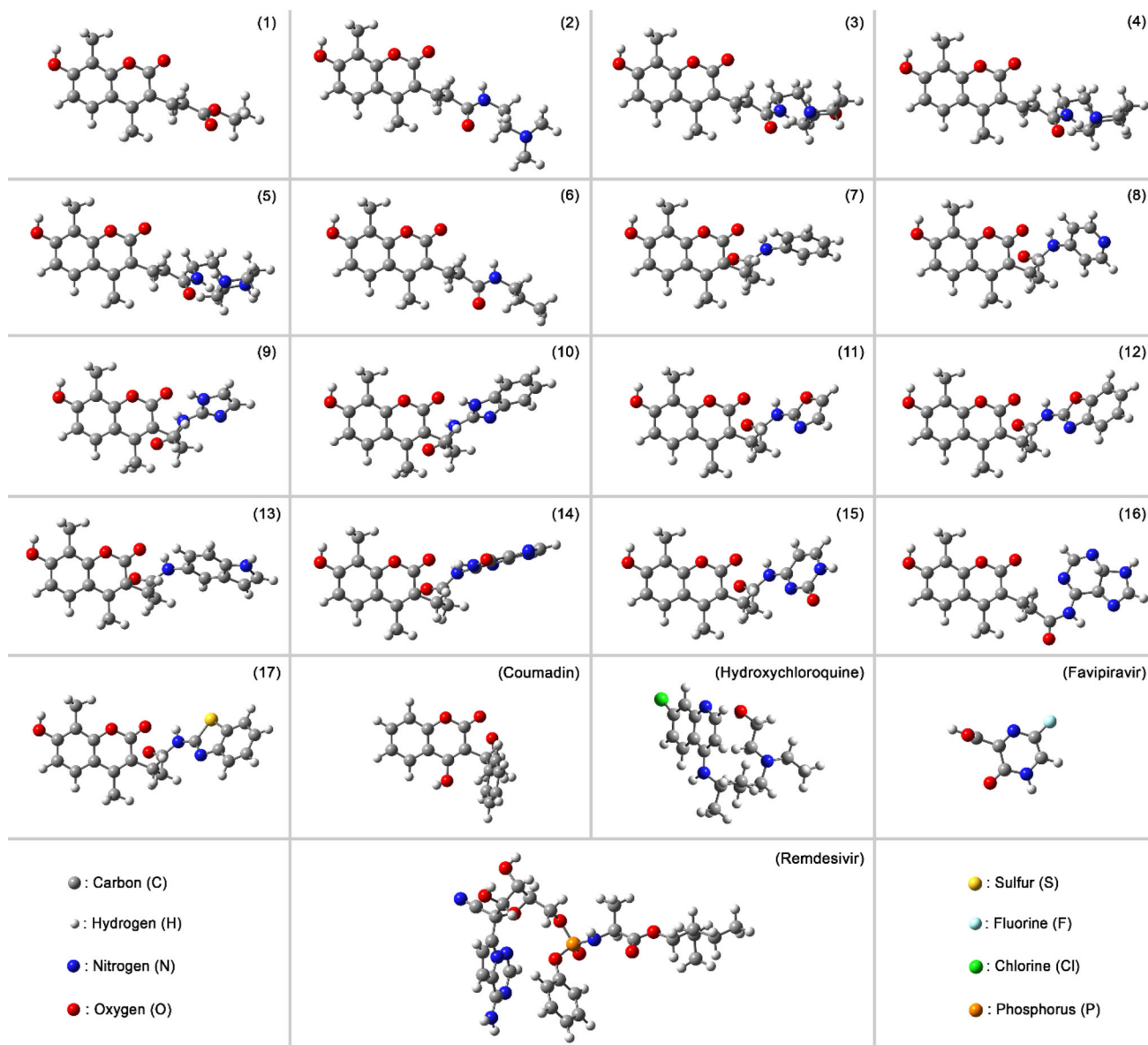
Figure 2. Three-dimensional optimized geometries of coumarins (**1**-**17**, warfarin, favipiravir, remdesivir, and hydroxychloroquine) obtained from DFT calculations.
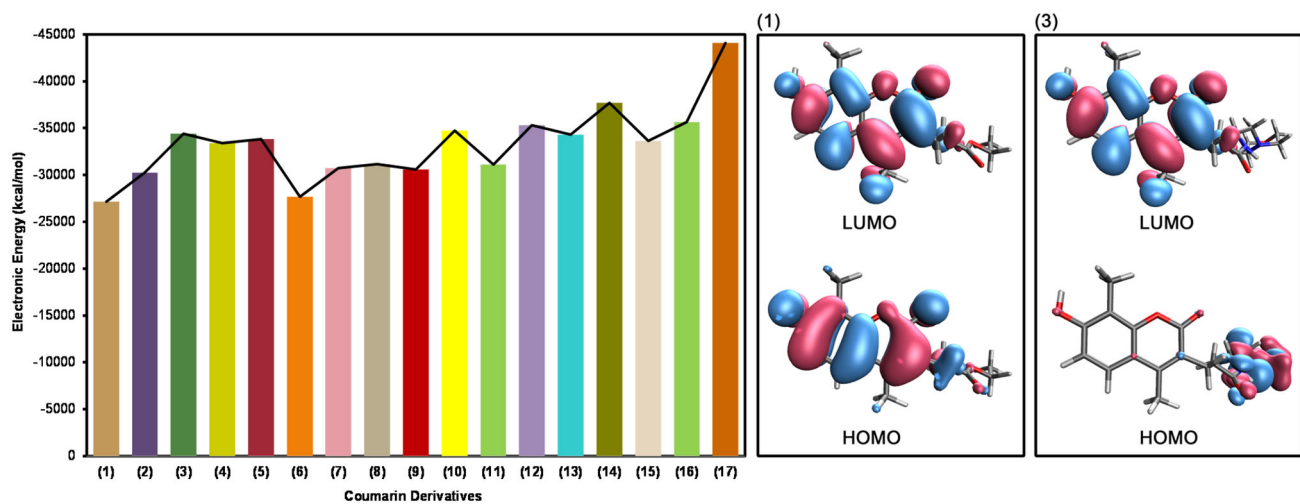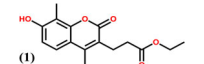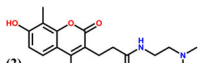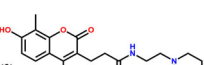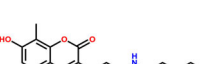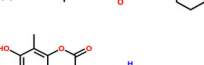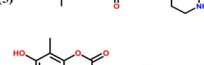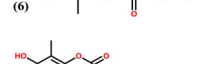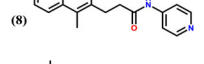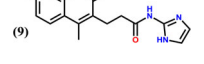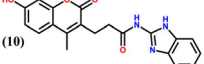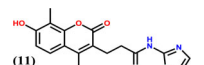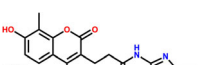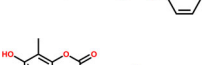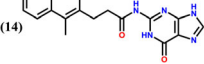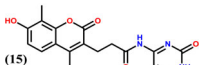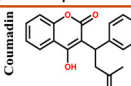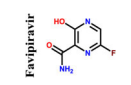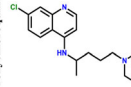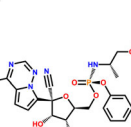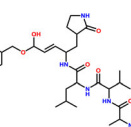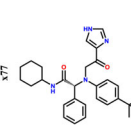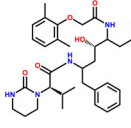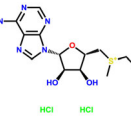

Figure 3. Comparative electronic energy diagram of coumarins (**1**-**17**) and molecule orbitals of **1** and **3**.

Table 1. Docking scores of coumarin derivatives (1-17) on SARS-CoV-2 receptors (7BQY3 for 3CLpro, 7BV23 for NSP12, 6WXC for NSP15, 6WKQ for NSP16, and 6M0J for Spike S1 subunit and ACE2 protein).

Target compounds	Docking scores								
	3CLPro	Spike-S1	ACE2	Spike-ACE2	NSP12	NSP12-RNA	NSP15	NSP16	VKORC1
(1)	−6.46	−5.85	−6.50	−6.14	−6.82	−7.12	−6.59	−6.51	−7.28
(2)	−7.07	−6.32	−7.05	−6.57	−8.58	−7.99	−7.03	−7.00	−7.93
(3)	−7.30	−6.74	−7.29	−7.28	−10.01 −(10.20)*	−8.30 −(9.62)*	−7.35	−7.00	−8.66 −(9.83)*
(4)	−7.35	−6.53	−7.31	−7.10	−8.70	−8.83	−7.45	−7.30	−8.61 −(9.91)*
(5)	−7.34	−6.71	−7.41	−7.03	−9.36 −(9.86)*	−9.10 −(9.33)*	−7.38	−7.18	−8.58 −(10.14)*
(6)	−6.83	−5.93	−6.66	−6.77	−7.12	−7.62	−6.76	−6.74	−7.58
(7)	−6.94	−6.14	−6.69	−6.48	−7.39	−7.57	−6.70	−6.93	−7.75
(8)	−6.88	−6.18	−6.94	−6.60	−7.51	−7.79	−6.87	−6.80	−7.77
(9)	−6.69	−6.01	−6.72	−6.65	−8.27	−8.83	−7.05	−6.66	−7.82
(10)	−7.25	−6.44	−7.32	−7.18	−8.91	−8.65	−7.09	−7.23	−8.22
(11)	−6.84	−6.26	−6.69	−6.52	−8.14	−8.29	−6.94	−6.86	−7.71
(12)	−7.30	−6.43	−7.38	−6.93	−8.05	−8.29	−7.17	−7.18	−8.25
(13)	−7.24	−6.53	−7.26	−7.02	−7.72	−7.95	−7.18	−7.10	−8.20
(14)	−7.47	−6.57	−7.47	−7.19	−8.81	−8.90	−7.20	−7.67	−8.35
(15)	−7.03	−6.18	−6.98	−6.55	−7.83	−7.92	−7.11	−7.00	−7.95
(16)	−7.33	−6.37	−7.15	−7.10	−9.09 −(10.10)*	−8.39 −(9.49)*	−7.15	−7.09	−8.28
(17)	−7.33	−6.40	−7.39	−7.28	−7.60	−8.10	−7.25	−7.38	−8.23

*Values obtained by energy minimization.

Table 2. Docking scores of reference compounds on SARS-CoV-2 receptors.

Target compounds	Docking scores								
	3CLPro	Spike-S1	ACE2	Spike-ACE2	NSP12	NSP12-RNA	NSP15	NSP16	VKORC1
Coumadin	−6.25	−5.45	−6.54	−5.91	−6.66 −(7.83)*	−7.06 −(7.88)*	−5.79	−6.35	−7.41 −(8.19)*
Favipiravir	−4.49	−3.97	−4.52	−4.97	−4.81 −(5.33)*	−4.85 −(5.43)*	−4.23	−4.87	−4.75
Hydroxychloroquine	−6.97	−5.96	−7.22	−6.68	−7.59 −(11.03)*	−7.92 −(11.12)*	−6.18	−6.89	−8.07
Remdesivir	−8.73	−7.50	−945	−8.59	−9.06 −(11.20)*	−9.51 −(12.61)*	−7.36	−8.65	−10.03 −(11.85)*
N3	−9.84	–	–	–	–	–	–	–	–
x77	−8.24	–	–	–	–	–	–	–	–
Lopinavir	–	–	–	–	–	–	−7.69	–	–
S-Adenosyl methionine	–	–	–	–	–	–	–	−8.13	–

*Values obtained by energy minimization.

(acceptor) interactions with compounds **2**, **9**, **12,** and **15**; backbone hydrogen bond (acceptor) interactions with compounds **2,491,015** and **17**; strong "arene attraction" with compounds **31,012** and **13**; weak "arene attraction" with compounds **5**, **7**, **9** and **14**. Pro620 residue shows strong arene attraction with compounds **121,415** and **17**, while weak arene attraction with compounds **25,910** and **13**.

The residues of the NSP12 protein that show the highest interaction with model compounds (warfarin, favipiravir, hydroxychloroquine, and remdesivir) are Arg555 and Arg553, respectively. Arg555 and Arg553 residues usually show strong sidechain hydrogen bond (acceptor) interaction in different docking poses of model (reference) compounds. When the different docking poses of coumarin compounds with NSP12 were examined together, it was observed that the Arg555 residue had strong sidechain hydrogen bond (acceptor) interactions with model compounds warfarin and remdesivir; strong arene attraction interaction with model compound hydroxychloroquine in only one docking pose. Arg553 residue shows sidechain hydrogen bond (acceptor)

interactions with all reference compounds in the different docking poses. At the same time, it was observed that warfarin and favipiravir created a strong arene attraction interaction with Ser682 residue of NSP12 protein.

While complex with the template and primary RNA components of NSP12 protein, the residues most frequently interacting with the coumarin compounds (**1**–**17**) are Arg555, Thr556, and Asp623, in docking calculations. The Arg555 residue generally shows side-chain hydrogen bond (acceptor) interactions with coumarin compounds series (except compounds **191,011** and **14**), weak arene attraction with compounds **23,414** and strong arene attraction interactions with compound **13**. The Thr556 and Asp623 residues generally show side-chain hydrogen bond (donor) interactions with the coumarin compounds (**1-17**) other than compounds **5**, **15**, and **17**. Strong metal ligation interactions are generally observed between the magnesium ions (especially the magnesium ion called MG1004 residue) and the coumarins (**1-17**), which are the natural components of NSP12 or NSP12-RNA complex. However, while the magnesium ions in
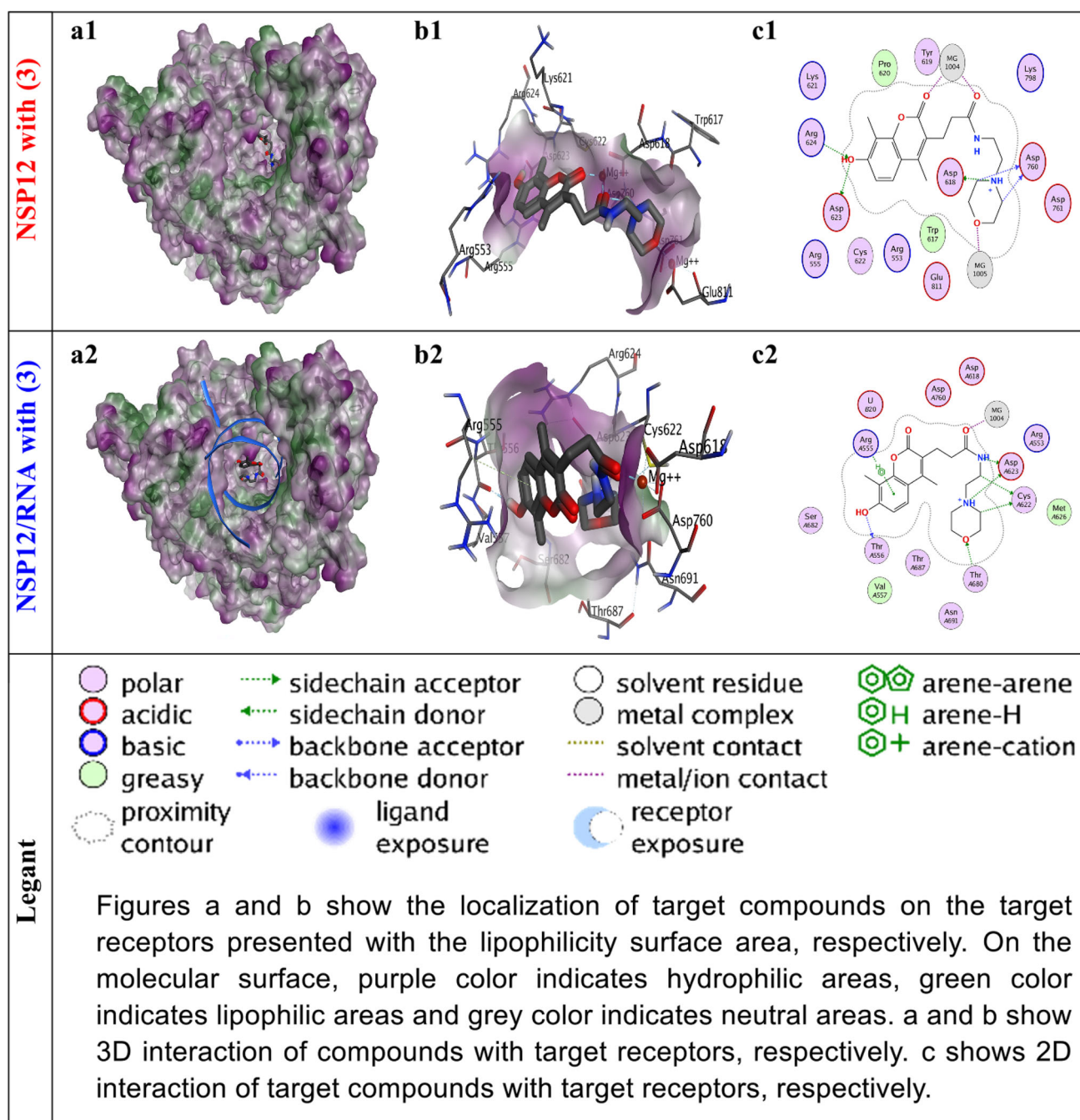
Figure 4. Docking results of compound **3** with NSP12 and NSP12-RNA complex.

the NSP12 and/or NSP12-RNA complex had no interaction with the reference molecules warfarin and favipiravir, it was observed that they formed strong interactions with the reference molecules hydroxychloroquine and remdesivir.

In docking analysis, the primary and template RNA components in the NSP12-RNA complex, especially template uracil nucleotide (t-U10) and the primary uracil nucleotide (p-U20), have strong molecular interactions with the coumarin derivatives (Figures 4 and 5).

The reference compound warfarin has established sidechain hydrogen bond (acceptor) interactions with Arg555, Ser759, t-U10, and p-U20 residues, and arene attraction interactions with Ser682 and p-U20 residues of the NSP-RNA

complex. Molecular interactions of other model compounds with the NSP12-RNA complex are given in Figures 4 and 5.

The protein-ligand docked complexes of the compounds **3**, **5**, and **16** with the highest docking scores were subjected to energy minimization. As a result of this process, the final docking scores of compounds **3**, **5**, and **16** were found to be −10.20, −9.86, and −10.10 kcal/mol, respectively (Figures 4 and 5). However, in docking analysis, the binding affinities of the model compounds warfarin, favipiravir, hydroxychloroquine, and remdesivir with the NSP12 protein were found to be −6.66, −4.81, −7.59, and −9.06 kcal/mol, respectively. When energy minimization was applied to the protein-ligand complexes obtained from the docking process of the model

Figure 5. Docking results of coumarins **5** and **16** with NSP12 and NSP12-RNA complex.

compounds with the NSP12 protein, the final docking scores of these compounds were found to be −7.83, −5.33, −11.03, and −11.20 kcal/mol, respectively (Figures S1–S4, Supporting material and Table 2).

In the coumarin compound series (**1**-**17**), the compounds with the highest docking score for the NSP12-RNA complex

were again **3**, **5, 16**, and their binding affinities were found as −9.10, −8.39, and −8.30 kcal/mol, respectively. The docking scores of these compounds as a result of energy minimization were found as −9.33, −9.49, and −9.62 kcal/mol, respectively (Table 1 and Figures 4, 5). In docking analysis, the binding affinities of the model compounds warfarin,

Figure 6. Docking results of coumarin **3**, **4**, **5**, and **warfarin** with VKORC1.

favipiravir, hydroxychloroquine, and remdesivir for the NSP12-RNA complex were found to be −7.06, −4.85, −7.92, and −9.51 kcal/mol, respectively. The docking scores of these compounds as a result of energy minimization were found as −7.88, −5.43, −11.12, and −12.61 kcal/mol, respectively

(Table 2 and Figures S1–S4, Supporting material). According to the docking results, with the exception of **3**, **5**, and **16**, both coumarin compounds (**1-17**) and selected model compounds generally bind to the NSP12-RNA complex with higher affinity than the NSP12 single protein. The specific

Table 3. The calculated binding energy (kcal/mol) and standard deviations of coumarins 3, 5, 16, and Remdesivir.

Time (ns)	Coumarin 3		Coumarin 5		Coumarin 16		Remdesivir	
	$\Delta G_{Binding}$	SD	$\Delta G_{Binding}$	SD	$\Delta G_{Binding}$	SD	$\Delta G_{Binding}$	SD
0	−72258.5	–	−72486.1	–	−72089.1	–	−89294.7	–
5	−56994.1	±4008.5	−56896.6	±4017.1	−54866.4	±4204.0	−68315.3	±5100.2
10	−57240.4	±333.1	−56092.3	±342.7	−54608.2	±267.4	−67549.7	±305.5
15	−57229.9	±220.6	−56550.1	±226.0	−54827.5	±228.6	−68228.7	±196.5
20	−55955.3	±500.3	−56241.5	±320.4	−53970.3	±412.3	−67304.5	±387.5
25	−56446.3	±260.0	−55944.1	±377.3	−54270.6	±316.8	−67185.4	±342.1
30	−56582.2	±247.7	−56470.9	±376.5	−54144.0	±382.1	−67401.0	±254.7
35	−57183.5	±273.8	−56896.4	±210.2	−54473.3	±374.6	−68138.7	±263.3
40	−57326.5	±292.6	−56889.7	±315.4	−54356.2	±305.1	−68243.2	±278.7
45	−55196.2	±706.0	−55640.3	±412.5	−53729.2	±248.1	−67378.9	±428.5
50	−56266.0	±456.6	−56704.1	±397.2	−54611.7	±472.6	−67536.8	±219.8
55	−56105.3	±249.8	−55992.7	±224.8	−53600.5	±407.1	−67199.7	±232.3
60	−56455.5	±307.1	−55582.9	±215.7	−54065.6	±254.3	−67112.6	±173.6
65	−55969.9	±274.0	−56513.5	±493.2	−54675.9	±280.1	−67154.2	±272.9
70	−56871.8	±357.5	−56042.5	±325.5	−53988.4	±323.4	−67654.7	±439.8
75	−55634.7	±416.6	−55783.2	±297.1	−54784.8	±215.3	−66944.8	±231.4
80	−55786.6	±421.4	−56091.4	±349.9	−54286.5	±333.6	−67572.0	±186.2
85	−56016.1	±323.2	−56057.1	±236.8	−54436.8	±460.9	−66855.1	±334.9
90	−56387.9	±438.7	−55840.7	±336.4	−54314.5	±458.0	−67156.0	±413.7
95	−56632.4	±243.5	−56124.1	±211.2	−54284.6	±236.3	−66950.1	±283.0
100	−56796.6	±347.9	−56396.1	±442.0	−54200.2	±386.4	−67526.2	±614.1
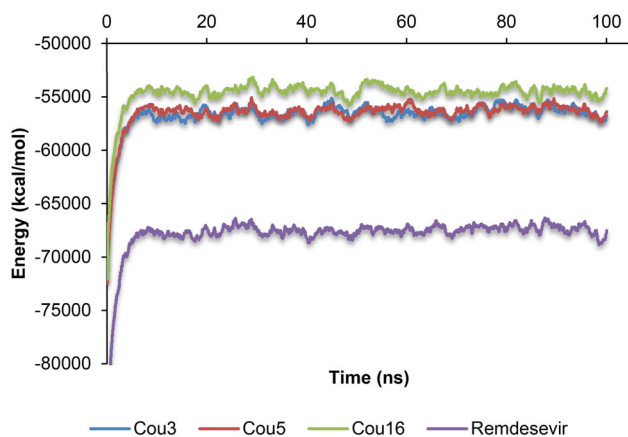
Figure 7. Change of Gibbs binding energies between 7BV2 and selected molecules in the range of 0–100 ns.

protein-ligand interactions of **3**, **5**, and **16** compounds are given in Figures 4 and 5.

Coumarin series compounds (**2-17**), except coumarin **1**, almost all gave a higher docking score against VKORC1 than the warfarin model compound. While the warfarin docking score was −7.41 kcal/mol, the coumarin derivatives (**2-17**) were observed to have binding affinities between −7.58 and −8.66 kcal/mol and higher energetic values than warfarin, except for coumarin **1**, which has a value of −7.28 kcal/mol. Another model compound, hydroxychloroquine, was observed to have a binding affinity of −8.07 kcal/mol with VKORC1. Nine coumarin derivatives gave a higher docking score against VKORC1 than the hydroxychloroquine model compound (Tables 1 and 2).

Possible interactions of other model inhibitors used in the study with VKORC1 were investigated by docking calculations (Figure 6). According to non-covalent docking calculations, "**Remdesivir**", an antiviral drug approved for use in European countries for the treatment of COVID-19, whose primary target is viral proteins, interestingly, showed a very high binding affinity for VKORC1 with −10.03 kcal/mol. The

clinical success of remdesivir against COVID-19 has suggested that both the compound's direct targeting of virus proteins and its anticoagulant effect may be important in secondary clinical situations (tables) developing after COVID-19 infection. We can suggest that it may be beneficial to address this situation in the clinical examinations of remdesivir related to COVID-19. Favipiravir is a compound that shows a covalent and irreversible inhibition mechanism with its primary target molecule. Therefore, a comparison of non-covalent docking scores would not be appropriate.

3.3. MM-PBSA analysis

Molecular docking has some disadvantages in the analysis of binding stability. In docking calculations, protein accepts as rigid while ligand accepts flexible. However, both protein and ligand are flexible in the living. The flexibility of both protein and ligand should be taken into consideration. For this aim, MM-PBSA calculations are performed for drug candidate, Coumarins **3**, **5**, **16** and Remdesivir. The binding energy is calculated in each 5 ns and given in Table 3. Additionally, standard deviation (SD) is calculated and given in same table.

The binding energies from 0 to 100 ns are calculated for selected complex structures. The energy values are represented in Figure 7.

According to Table 3 and Figure 7, it can be said that selected drug candidates are effective against RNA dependent RNA polymerase (RdRp). However, the most effective one is remdesivir in the inhibition of NSP12 which is RdRp. Also, coumarin **3** and coumarin **5** have similar effectivity and their activities are better than coumarin **16**. The complex structure between coumarin **3** and 7BV2 at 0,255,075 and 100 ns are represented in Figure 8.
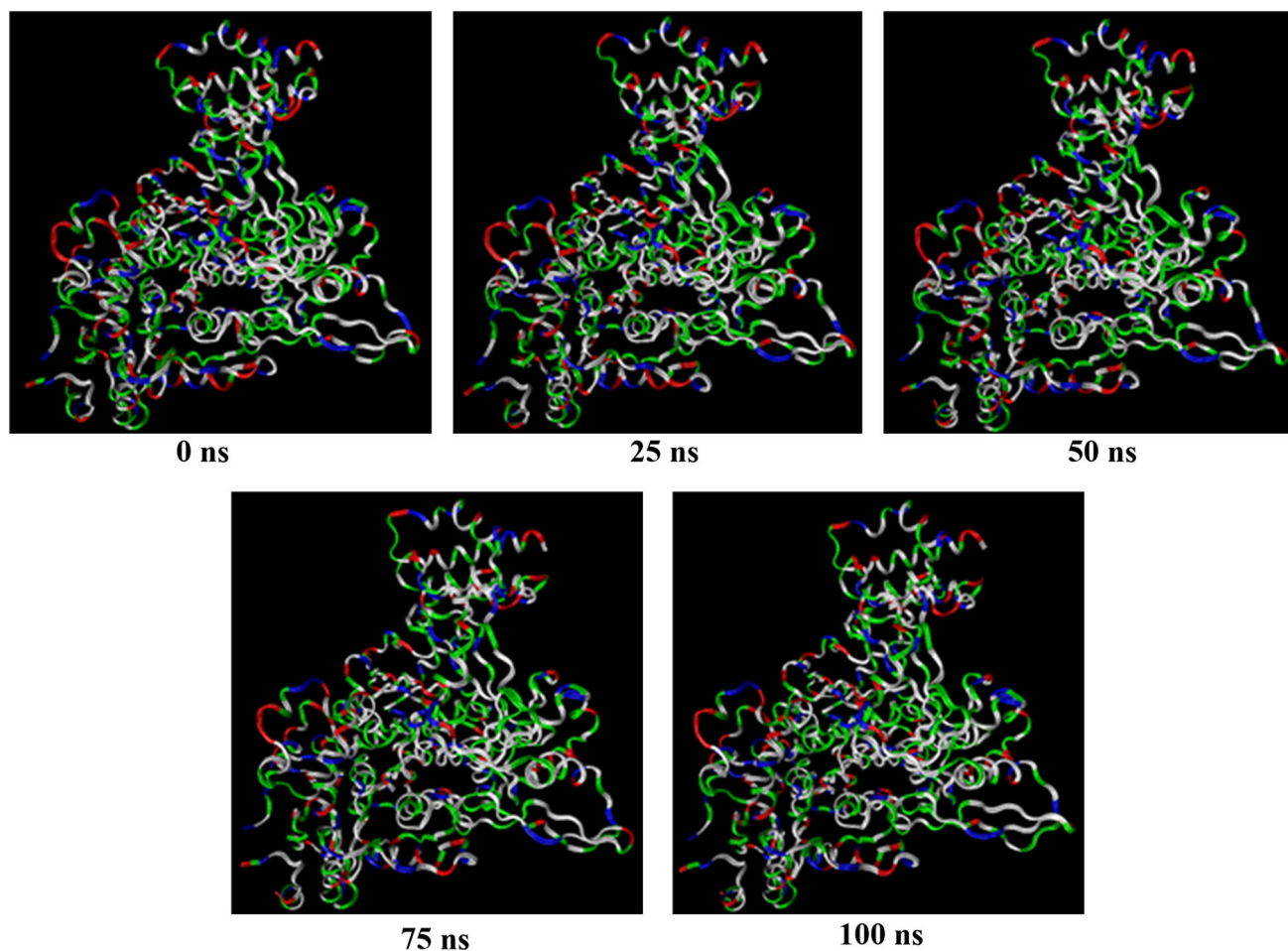
Figure 8. The coumarin **3**-7BV2 complex structure at different times (0–100 ns).

4. Conclusion

In this study, coumarin derivatives containing secondary amine substituents were designed to develop effective antiviral agents to inhibit coronavirus. DFT method was used to estimate the ideal geometries and physicochemical properties of molecules. 17 coumarin derivatives were studied using molecular docking studies against MPro, NSP12 with RNA, NSP15, NSP16, and Spike with ACE2, which are important receptors of SARS-CoV-2, and their binding scores were compared with those of warfarin, favipiravir, remdesivir, and hydroxychloroquine model inhibitors. The coumarin series was found to be specific for NSP12 among all receptors, and the highest scores were obtained for NSP12 or NSP12/RNA. In the coumarin series, the compounds with the highest docking score for the NSP12-RNA complex were again **5**, **16**, and **3**, and their binding affinities were found as −9.10, −8.39, and −8.30 kcal/mol, respectively. These scores are higher than the binding affinities of warfarin, favipiravir, and hydroxychloroquine, but lower than the binding affinity of remdesivir. These differences in docking calculation results between the coumarin compounds (**1**–**17**) and the main reference molecule warfarin, and it is thought that the coumarin compounds (**1**–**17**) may be more active than warfarin. Since coronavirus is known to cause pulmonary embolism, binding affinities against vitamin K epoxide reductase complex inhibitor have also been investigated, taking into account the anticoagulant property, which is an important property of coumarins. Other coumarins, except the amine-free starting coumarin, scored better than the blood-thinning drug warfarin, but again remdesivir scored best against the vitamin K epoxide reductase complex. In conclusion, the coumarin series in this study is specific against NSP12 and viral replication can be prevented by inhibition of this enzyme. Coumarins with high binding scores are suitable compounds for new designs and organic reactions, and new designs may be made using the functional groups of remdesivir compound and will be promising for the development of multifunctional and powerful antiviral drugs. MM-PBSA calculations are performed and it is found that coumarin **3**, **5**, and **16** are found as active against 7BV2. These ligands are in a stable interaction.

Disclosure statement

ORCID

Mücahit Özdemir (iD) http://orcid.org/0000-0002-0840-4953
Baybars Köksoy (iD) http://orcid.org/0000-0001-7939-5380
Deniz Ceyhan (iD) http://orcid.org/0000-0003-1811-3858
Koray Sayın (iD) http://orcid.org/0000-0001-6648-5010
Erol Erçağ (iD) http://orcid.org/0000-0003-4927-2405
Mustafa Bulut (iD) http://orcid.org/0000-0001-9598-2649
Bahattin Yalçın (iD) http://orcid.org/0000-0003-4448-1101

References

Abuknesha, R. A., & Darwish, F. (2005). Coupling of enzymatic and immunoassay steps to detect *E. coli*: A new, highly sensitive tandem technique for the analysis of low levels of bacteria. *Talanta*, 65(2), 343–348. https://doi.org/10.1016/j.talanta.2004.07.007

Aktaş, A., Tüzün, B., Aslan, R., Sayin, K., & Ataseven, H. (2020). New anti-viral drugs for the treatment of COVID-19 instead of favipiravir. *Journal of Biomolecular Structure and Dynamics*, 1–11. https://doi.org/10.1080/07391102.2020.1806112

Al-Tawfiq, J. A. (2020). Asymptomatic coronavirus infection: MERS-CoV and SARS-CoV-2 (COVID-19). *Travel Medicine and Infectious Disease*, 35, 101608. https://doi.org/10.1016/j.tmaid.2020.101608

Barnes, G. D., Burnett, A., Allen, A., Blumenstein, M., Clark, N. P., Cuker, A., Dager, W. E., Deitelzweig, S. B., Ellsworth, S., Garcia, D., Kaatz, S., & Minichiello, T. (2020). Thromboembolism and anticoagulant therapy during the COVID-19 pandemic: Interim clinical guidance from the anticoagulation forum. *Journal of Thromb Thrombolysis*, 50(1), 72–81. https://doi.org/10.1007/s11239-020-02138-z

Becke, A. D. (1988). Density-functional exchange-energy approximation with correct asymptotic behavior. *Physical Review A: General Physics*, 38(6), 3098–3100. https://doi.org/10.1103/physreva.38.3098

Becke, A. D. (1993). Becke's three parameter hybrid method using the LYP correlation functional. *The Journal of Chemical Physics*, 98(7), 5648–5652. https://doi.org/10.1063/1.464913

Beigel, J. H., Tomashek, K. M., Dodd, L. E., Mehta, A. K., Zingman, B. S., Kalil, A. C., Hohmann, E., Chu, H. Y., Luetkemeyer, A., Kline, S., Lopez de Castilla, D., Finberg, R. W., Dierberg, K., Tapson, V., Hsieh, L., Patterson, T. F., Paredes, R., Sweeney, D. A., Short, W. R., … Lane, C. H. (2020). Remdesivir for the treatment of Covid-19—Final report. *New England Journal of Medicine*, 383(19), 1813–1826. https://doi.org/10.1056/NEJMoa2007764

Berman, H. M., Westbrook, J., Feng, Z., Gilliland, G., Bhat, T. N., Weissig, H., Shindyalov, I. N., & Bourne, P. E. (2000). The protein data bank. *Nucleic Acids Research*, 28(1), 235–242. https://doi.org/10.1093/nar/28.1.235

Bienert, S., Waterhouse, A., de Beer, T. A., Tauriello, G., Studer, G., Bordoli, L., & Schwede, T. (2017). The SWISS-MODEL repository-new features and functionality. *Nucleic Acids Research*, 45(D1), D313–D319. https://doi.org/10.1093/nar/gkw1132

Cai, Q., Yang, M., Liu, D., Chen, J., Shu, D., Xia, J., Liao, X., Gu, Y., Cai, Q., Yang, Y., Shen, C., Li, X., Peng, L., Huang, D., Zhang, J., Zhang, S., Wang, F., Liu, J., Chen, L., … Liu, L. (2020). Experimental treatment with favipiravir for COVID-19: An open-label control study. *Engineering*, 6(10), 1192–1198. https://doi.org/10.1016/j.eng.2020.03.007

Cao, Y., Li, L., Feng, Z., Wan, S., Huang, P., Sun, X., Wen, F., Huang, X., Ning, G., & Wang, W. (2020). Comparative genetic analysis of the novel coronavirus (2019-nCoV/SARS-CoV-2) receptor ACE2 in different populations. *Cell Discovery*, 6(11), 11–14. https://doi.org/10.1038/s41421-020-0147-1

Case, D. A., Darden, T. A., Cheatham, T. E., III, Simmerling, C. L., Wang, J., Duke, R. E., Luo, R., Walker, R. C., Zhang, W., Merz, K. M., Roberts, B., Hayik, S., Roitberg, A., Seabra, G., Swails, J., Götz, A. W., Kolossváry, I., Wong, K. F., Paesani, F., … Kollman, P. A. (2012). AMBER 12. University of California, San Francisco.

Casey, K., Iteen, A., Nicolini, R., & Auten, J. (2020). COVID-19 pneumonia with hemoptysis: Acute segmental pulmonary emboli associated with novel coronavirus infection. *The American Journal of Emergency Medicine*, 38(7), 1544.e1–1544.e1543. https://doi.org/10.1016/j.ajem.2020.04.011

ChemAxon (2016). MarvinSketch: Marvin was used for drawing, displaying and characterizing chemical structures, substructures and reactions (Version Marvin 16.12.12).

Chikhale, R. V., Sinha, S. K., Patil, R. B., Prasad, S. K., Shakya, A., Gurav, N., Prasad, R., Dhaswadikar, S. R., Wanjari, M., & Gurav, S. S. (2020). In-silico investigation of phytochemicals from Asparagus racemosus as plausible antiviral agent in COVID-19. *Journal of Biomolecular Structure and Dynamics*, 1–15. https://doi.org/10.1080/07391102.2020.1784289

Consortium, T. U. (2019). UniProt: A worldwide hub of protein knowledge. *Nucleic Acids Research*, 47(D1), D506–D515. https://doi.org/10.1093/nar/gky1049

Czogalla, K. J., Watzka, M., & Oldenburg, J. (2015). Structural modeling insights into human VKORC1 phenotypes. *Nutrients*, 7(8), 6837–6851. https://doi.org/10.3390/nu7085313

da Silva Antonio, A., Wiedemann, L. S. M., & Veiga-Junior, V. F. (2020). Natural products' role against COVID-19. *RSC Advances*, 10(39), 23379–23393. https://doi.org/10.1039/D0RA03774E

de Souza, S. M., Delle Monache, F., & Smânia, A. (2005). Antibacterial activity of coumarins. *Zeitschrift Fur Naturforschung. C: Journal of Biosciences*, 60(9–10), 693–700. https://doi.org/10.1515/znc-2005-9-1006

Dennington, R., Keith, T., & Millam, J. (2009). GaussView (Version 5.0).

Donoghue, M., Hsieh, F., Baronas, E., Godbout, K., Gosselin, M., Stagliano, N., Donovan, M., Woolf, B., Robison, K., Jeyaseelan, R., Breitbart, R. E., & Acton, S. (2000). A novel angiotensin-converting enzyme–related carboxypeptidase (ACE2) converts angiotensin I to angiotensin. *Circulation Research*, 87(5), 1–9.e1–e9. https://doi.org/10.1161/01.RES.87.5.e1

Edelsbrunner, H., & Mücke, E. P. (1994). Three-dimensional alpha shapes. *ACM Transactions on Graphics*, 13(1), 43–72. https://doi.org/10.1145/174462.156635

Fang, L., Karakiulakis, G., & Roth, M. (2020). Are patients with hypertension and diabetes mellitus at increased risk for COVID-19 infection? *The Lancet Respiratory Medicine*, 8(4), e21. https://doi.org/10.1016/S2213-2600(20)30116-8

Frisch, M. J., Trucks, G. W., Schlegel, H. B., Scuseria, G. E., Robb, M. A., Cheeseman, J. R., Scalmani, G., Barone, V., Mennucci, B., Petersson, G. A., Nakatsuji, H., Caricato, M., Li, X., Hratchian, H. P., Izmaylov, A. F., Bloino, J., Zheng, G., Sonnenberg, J. L., Hada, M., … Fox, D. J. (2009). *Gaussian 09 Revision C. 01*. Gaussian, Inc.

Ganatra, S., Hammond, S. P., & Nohria, A. (2020). The novel coronavirus disease (COVID-19) threat for patients with cardiovascular disease and cancer. *JACC Cardiooncology*, 2(2), 350–355. https://doi.org/10.1016/j.jaccao.2020.03.001

Gautret, P., Lagier, J.-C., Parola, P., Hoang, V. T., Meddeb, L., Mailhe, M., Doudier, B., Courjon, J., Giordanengo, V., Vieira, V. E., Tissot Dupont, H., Honoré, S., Colson, P., Chabrière, E., La Scola, B., Rolain, J.-M., Brouqui, P., & Raoult, D. (2020). Hydroxychloroquine and azithromycin as a treatment of COVID-19: Results of an open-label non-randomized clinical trial. *International Journal of Antimicrobial Agents*, 56(1), 105949. https://doi.org/10.1016/j.ijantimicag.2020.105949

Geleris, J., Sun, Y., Platt, J., Zucker, J., Baldwin, M., Hripcsak, G., Labella, A., Manson, D. K., Kubin, C., Barr, R. G., Sobieszczyk, M. E., & Schluger, N. W. (2020). Observational study of hydroxychloroquine in hospitalized patients with Covid-19. *New England Journal of Medicine*, 382(25), 2411–2418. https://doi.org/10.1056/NEJMoa2012410

Gerber, P. R., & Müller, K. (1995). MAB, a generally applicable molecular force field for structure modelling in medicinal chemistry. *Journal of Computer Aided Molecular Design*, 9(3), 251–268. https://doi.org/10.1007/BF00124456

Ghebreyesus, T. A. (2020). *WHO Director-General's opening remarks at the media briefing on COVID-19-11 March 2020*. World Health Organization.

Gorbalenya, A. E., Baker, S. C., Baric, R. S., Groot, R. J. d., Drosten, C., Gulyaeva, A. A., Haagmans, B. L., Lauber, C., Leontovich, A. M., Neuman, B. W., Penzar, D., Perlman, S., Poon, L. L. M., Samborskiy, D. V., Sidorov, I. A., Sola, I., & Ziebuhr, J. (2020). The species severe acute respiratory syndrome-related coronavirus: Classifying 2019-nCoV and naming it SARS-CoV-2. *Nature Microbiology*, 5(4), 536. https://doi.org/10.1038/s41564-020-0695-z

Grein, J., Ohmagari, N., Shin, D., Diaz, G., Asperges, E., Castagna, A., Feldt, T., Green, G., Green, M. L., Lescure, F.-X., Nicastri, E., Oda, R., Yo, K., Quiros-Roldan, E., Studemeister, A., Redinski, J., Ahmed, S., Bernett, J., Chelliah, D., … Flanigan, T. (2020). Compassionate use of remdesivir for patients with severe Covid-19. *New England Journal of Medicine*, 382(24), 2327–2336. https://doi.org/10.1056/NEJMoa2007016

Guo, Y.-R., Cao, Q.-D., Hong, Z.-S., Tan, Y.-Y., Chen, S.-D., Jin, H.-J., Tan, K.-S., Wang, D.-Y., & Yan, Y. (2020). The origin, transmission and clinical therapies on coronavirus disease 2019 (COVID-19) outbreak–an update on the status. *Military Medical Research*, 7(1), 1–10. https://doi.org/10.1186/s40779-020-00240-0

Halgren, T. A. (1996). Merck molecular force field. I. Basis, form, scope, parameterization, and performance of MMFF94. *Journal of Computational Chemistry*, 17(5–6), 490–519. https://doi.org/10.1002/(SICI)1096-987X(199604)17:5/6<490::AID-JCC1>3.0.CO;2-P

Hamming, I., Timens, W., Bulthuis, M., Lely, A., Navis, G. V., & van Goor, H. (2004). Tissue distribution of ACE2 protein, the functional receptor for SARS coronavirus. A first step in understanding SARS pathogenesis. *The Journal of Pathology*, 203(2), 631–637. https://doi.org/10.1002/path.1570

Hassan, M. Z., Osman, H., Ali, M. A., & Ahsan, M. J. (2016). Therapeutic potential of coumarins as antiviral agents. *European Journal of Medicinal Chemistry*, 123, 236–255. https://doi.org/10.1016/j.ejmech.2016.07.056

Hoffmann, M., Kleine-Weber, H., Schroeder, S., Krüger, N., Herrler, T., Erichsen, S., Schiergens, T. S., Herrler, G., Wu, N.-H., Nitsche, A., Müller, M. A., Drosten, C., & Pöhlmann, S. (2020). SARS-CoV-2 cell entry depends on ACE2 and TMPRSS2 and is blocked by a clinically proven protease inhibitor. *Cell*, 181(2), 271–280. e278. https://doi.org/10.1016/j.cell.2020.02.052

Huang, C., Wang, Y., Li, X., Ren, L., Zhao, J., Hu, Y., Zhang, L., Fan, G., Xu, J., Gu, X., Cheng, Z., Yu, T., Xia, J., Wei, Y., Wu, W., Xie, X., Yin, W., Li, H., Liu, M., … Cao, B. (2020). Clinical features of patients infected with 2019 novel coronavirus in Wuhan, China. *The Lancet*, 395(10223), 497–506. https://doi.org/10.1016/S0140-6736(20)30183-5

Humphrey, W., Dalke, A., & Schulten, K. (1996). VMD: Visual molecular dynamics. *Journal of Molecular Graphics*, 14(1), 33–37. https://doi.org/10.1016/0263-7855(96)00018-5

Jin, Z., Du, X., Xu, Y., Deng, Y., Liu, M., Zhao, Y., Zhang, B., Li, X., Zhang, L., Peng, C., Duan, Y., Yu, J., Wang, L., Yang, K., Liu, F., Jiang, R., Yang, X., You, T., Liu, X., … Yang, H. (2020). Structure of Mpro from SARS-CoV-2 and discovery of its inhibitors. *Nature*, 582(7811), 289–285. https://doi.org/10.1038/s41586-020-2223-y

Jordan, R. E., Adab, P., & Cheng, K. (2020). Covid-19: Risk factors for severe disease and death. *British Medical Journal Publishing Group*, 368(m1198), 1–2. https://doi.org/10.1136/bmj.m1198

Keidar, S., Kaplan, M., & Gamliel-Lazarovich, A. (2007). ACE2 of the heart: From angiotensin I to angiotensin (1–7). *Cardiovascular Research*, 73(3), 463–469. https://doi.org/10.1016/j.cardiores.2006.09.006

Kim, Y., Jedrzejczak, R., Maltseva, N. I., Wilamowski, M., Endres, M., Godzik, A., Michalska, K., & Joachimiak, A. (2020). Crystal structure of Nsp15 endoribonuclease NendoU from SARS-CoV-2. *Protein Science*, 29(7), 1596–1605. https://doi.org/10.1002/pro.3873

Koch-Weser, J., & Sellers, E. M. (1971). Drug interactions with coumarin anticoagulants. *New England Journal of Medicine*, 285(10), 547–558. https://doi.org/10.1056/NEJM197109022851005

Kohn, W., & Sham, L. J. (1965). Self-consistent equations including exchange and correlation effects. *Physical Review*, 140(4A), A1133–A1138. https://doi.org/10.1103/PhysRev.140.A1133

Kollman, P. A., Massova, I., Reyes, C., Kuhn, B., Huo, S., Chong, L., Lee, M., Lee, T., Duan, Y., Wang, W., Donini, O., Cieplak, P., Srinivasan, J., Case, D. A., & Cheatham, T. E. (2000). Calculating structures and free energies of complex molecules: Combining molecular mechanics and

continuum models. *Accounts of Chemical Research*, 33(12), 889–897. https://doi.org/10.1021/ar000033j

Kreutz, R., Algharably, E. A. E.-H., Azizi, M., Dobrowolski, P., Guzik, T., Januszewicz, A., Persu, A., Prejbisz, A., Riemer, T. G., Wang, J.-G., & Burnier, M. (2020). Hypertension, the renin–angiotensin system, and the risk of lower respiratory tract infections and lung injury: Implications for COVID-19 European Society of Hypertension COVID-19 Task Force Review of Evidence. *Cardiovascular Research*, 116(10), 1688–1699. https://doi.org/10.1093/cvr/cvaa097

Kumar, A., Choudhir, G., Shukla, S. K., Sharma, M., Tyagi, P., Bhushan, A., & Rathore, M. (2020). Identification of phytochemical inhibitors against main protease of COVID-19 using molecular modeling approaches. *Journal of Biomolecular Structure and Dynamics*, 1–11. https://doi.org/10.1080/07391102.2020.1772112

Labute, P. (2007). *Protonate 3D: Assignment of macromolecular protonation state and geometry* (pp. 1–17). Chemical Computing Group Inc.

Lan, J., Ge, J., Yu, J., Shan, S., Zhou, H., Fan, S., Zhang, Q., Shi, X., Wang, Q., Zhang, L., & Wang, X. (2020). Structure of the SARS-CoV-2 spike receptor-binding domain bound to the ACE2 receptor. *Nature*, 581(7807), 215–220. https://doi.org/10.1038/s41586-020-2180-5

Lee, C., Yang, W., & Parr, R. G. (1988). Development of the Colle-Salvetti correlation-energy formula into a functional of the electron density. *Physical Review B*, 37(2), 785–789. https://doi.org/10.1103/PhysRevB.37.785

Lu, H., Stratton, C. W., & Tang, Y. W. (2020). Outbreak of pneumonia of unknown etiology in Wuhan, China: The mystery and the miracle. *Journal of Medical Virology*, 92(4), 401–402. https://doi.org/10.1002/jmv.25678

Minasov, G., Shuvalova, L., Rosas-Lemus, M., Kiryukhina, O., & Satchell, K. J. F. (2020). 1.98 Angstrom resolution crystal structure of NSP16-NSP10 heterodimer from SARS-CoV-2 in complex with sinefungin. *RCSB Pdb*, https://doi.org/10.2210/pdb6wkq/pdb.

Murray, R. D. H., Méndez, J., & Brown, S. A. (1982). *The natural coumarins: Occurrence, chemistry, and biochemistry*. John Wiley and Sons.

Nelson, M. T., Humphrey, W., Gursoy, A., Dalke, A., Kalé, L. V., Skeel, R. D., & Schulten, K. (1996). NAMD: A parallel, object-oriented molecular dynamics program. *The International Journal of Supercomputer Applications and High Performance Computing*, 10(4), 251–268. https://doi.org/10.1177/109434209601000401

Oldenburg, J., Bevans, C. G., Müller, C. R., & Watzka, M. (2006). Vitamin K epoxide reductase complex subunit 1 (VKORC1): The key protein of the vitamin K cycle. *Antioxidants & Redox Signaling*, 8(3–4), 347–353. https://doi.org/10.1089/ars.2006.8.347

Pandey, P., Rane, J. S., Chatterjee, A., Kumar, A., Khan, R., Prakash, A., & Ray, S. (2020). Targeting SARS-CoV-2 spike protein of COVID-19 with naturally occurring phytochemicals: An in silico study for drug development. *Journal of Biomolecular Structure and Dynamics*, 1–11. https://doi.org/10.1080/07391102.2020.1796811

Parks, J. M., & Smith, J. C. (2020). How to discover antiviral drugs quickly. *New England Journal of Medicine*, 382(23), 2261–2264. https://doi.org/10.1056/NEJMcibr2007042

Pires, D. E., Blundell, T. L., & Ascher, D. B. (2015). pkCSM: Predicting small-molecule pharmacokinetic and toxicity properties using graph-based signatures. *Journal of Medicinal Chemistry*, 58(9), 4066–4072. https://doi.org/10.1021/acs.jmedchem.5b00104

Sashidhara, K. V., Kumar, A., Kumar, M., Sarkar, J., & Sinha, S. (2010). Synthesis and in vitro evaluation of novel coumarin-chalcone hybrids as potential anticancer agents. *Bioorganic & Medicinal Chemistry Letters*, 20(24), 7205–7211. https://doi.org/10.1016/j.bmcl.2010.10.116

Singhal, T. (2020). A review of coronavirus disease-2019 (COVID-19). *Indian Journal of Pediatrics*, 87(4), 281–286. https://doi.org/10.1007/s12098-020-03263-6

Thakur, A., Singla, R., & Jaitak, V. (2015). Coumarins as anticancer agents: A review on synthetic strategies, mechanism of action and SAR studies. *European Journal of Medicinal Chemistry*, 101, 476–495. https://doi.org/10.1016/j.ejmech.2015.07.010

Ul Qamar, M. T., Alqahtani, S. M., Alamri, M. A., & Chen, L.-L. (2020). Structural basis of SARS-CoV-2 3CLpro and anti-COVID-19 drug discovery from medicinal plants. *Journal of Pharmaceutical Analysis*, 10(4), 313–319. https://doi.org/10.1016/j.jpha.2020.03.009

ULC, C. C. G. (2019). *Molecular operating environment (MOE) (Version 2019.01)*.

Viswanathan, T., Arya, S., Chan, S.-H., Qi, S., Dai, N., Misra, A., Park, J.-G., Oladunni, F., Kovalskyy, D., Hromas, R. A., Martinez-Sobrido, L., & Gupta, Y. K. (2020). Structural basis of RNA cap modification by SARS-CoV-2. *Nature Communications*, *11*(1), 3718. https://doi.org/10.1038/s41467-020-17496-8

Wang, Q., Wu, J., Wang, H., Gao, Y., Liu, Q., Mu, A., Ji, W., Yan, L., Zhu, Y., Zhu, C., Fang, X., Yang, X., Huang, Y., Gao, H., Liu, F., Ge, J., Sun, Q., Yang, X., Xu, W., ... Rao, Z. (2020). Structural basis for RNA replication by the SARS-CoV-2 polymerase. *Cell*, *182*(2), 417–428. e413. https://doi.org/10.1016/j.cell.2020.05.034

Wang, X., Fang, X., Cai, Z., Wu, X., Gao, X., Min, J., & Wang, F. (2020). Comorbid chronic diseases and acute organ injuries are strongly correlated with disease severity and mortality among COVID-19 patients: A systemic review and meta-analysis. *Research (Washington, D.C.)*, *2020*, 2402961. https://doi.org/10.34133/2020/2402961

Wang, Y., Zhang, D., Du, G., Du, R., Zhao, J., Jin, Y., Fu, S., Gao, L., Cheng, Z., Lu, Q., Hu, Y., Luo, G., Wang, K., Lu, Y., Li, H., Wang, S., Ruan, S., Yang, C., Mei, C., ... Wang, C. (2020). Remdesivir in adults with severe COVID-19: A randomised, double-blind, placebo-controlled, multi-centre trial. *The Lancet*, *395*(10236), 1569–1578. https://doi.org/10.1016/S0140-6736(20)31022-9

Wu, C., Liu, Y., Yang, Y., Zhang, P., Zhong, W., Wang, Y., Wang, Q., Xu, Y., Li, M., Li, X., Zheng, M., Chen, L., & Li, H. (2020). Analysis of therapeutic targets for SARS-CoV-2 and discovery of potential drugs by computational methods. *Acta Pharmaceutica Sinica B*, *10*(5), 766–788. https://doi.org/10.1016/j.apsb.2020.02.008

Yin, W., Mao, C., Luan, X., Shen, D.-D., Shen, Q., Su, H., Wang, X., Zhou, F., Zhao, W., Gao, M., Chang, S., Xie, Y.-C., Tian, G., Jiang, H.-W., Tao, S.-C., Shen, J., Jiang, Y., Jiang, H., Xu, Y., ... Xu, H. E. (2020). Structural basis for inhibition of the RNA-dependent RNA polymerase from SARS-CoV-2 by remdesivir. *Science (New York, N.Y.)*, *368*(6498), 1499–1504. https://doi.org/10.1126/science.abc1560

Zheng, Y.-Y., Ma, Y.-T., Zhang, J.-Y., & Xie, X. (2020). COVID-19 and the cardiovascular system. *Nature Reviews Cardiology*, *17*(5), 259–260. https://doi.org/10.1038/s41569-020-0360-5

Zu, Z. Y., Jiang, M. D., Xu, P. P., Chen, W., Ni, Q. Q., Lu, G. M., & Zhang, L. J. (2020). Coronavirus disease 2019 (COVID-19): A perspective from China. *Radiology*, *296*(2), E15–E25. https://doi.org/10.1148/radiol.2020200490